

## A lattice-gas model for alkali-metal fullerenes: body-centred-cubic structure

To cite this article: György Szabó and László Udvardi 1998 *J. Phys.: Condens. Matter* **10** 4211

View the [article online](#) for updates and enhancements.

### You may also like

- [Ac impedance of  \$A\_4C\_{60}\$  fullerenes under pressure](#)  
Bertil Sundqvist, Ove Andersson, Chen Gong et al.
- [Superconductivity of fullerenes with composition  \$A\_nIn\_xGa\_yC\_{60}\$  \( \$A=K,Rb,Cs\$ ;  \$n=2,3\$ \) synthesized from gallams](#)  
V A Kulbachinskii, B M Bulychev, R A Lunin et al.
- [Exotic s-wave superconductivity in alkali-doped fullerenes](#)  
Yusuke Nomura, Shiro Sakai, Massimo Capone et al.



**IOP | ebooks™**

Bringing together innovative digital publishing with leading authors from the global scientific community.

Start exploring the collection—download the first chapter of every title for free.

## A lattice-gas model for alkali-metal fullerenes: body-centred-cubic structure

György Szabó† and László Udvardi‡

† Research Institute for Technical Physics and Materials Science, H-1525 Budapest, POB 49, Hungary

‡ Quantum Theory Group, Institute of Physics, Technical University of Budapest, H-1111 Budapest, Budafoki út 8, Hungary

Received 30 January 1998

**Abstract.** A Coulomb lattice-gas model with a host-lattice screening mechanism is adapted to describe the ordering phenomena in alkali-metal fullerenes of body-centred-cubic structure. It is assumed that the electric charge of an alkali ion residing at a tetrahedral interstitial site is completely screened by its first-neighbour  $C_{60}$  molecules. The electronic energy of the  $C_{60}^{x-}$  ion is also taken into consideration as a charged spherical shell. By means of these assumptions an effective (short-range) pair interaction between two alkali ions is obtained. The resultant lattice-gas model is analysed by using two- and six-sublattice mean-field approximations. The thermodynamic properties are summarized in phase diagrams for different shell radii.

### 1. Introduction

In a previous paper [1] (henceforth referred to as I) we have introduced a lattice-gas model to describe the ordering of alkali atoms intercalated into solid  $C_{60}$  of face-centred-cubic (FCC) structure. This model is now adapted to a body-centred-cubic (BCC) host, in view of the fact that these structures are also observed in experiments (see the reviews in references [2, 3]).

Lattice-gas (Ising) models provide an adequate description of ordering phenomena in intercalated alloys. Difficulties arise, however, when determining the effective pair interaction between two intercalated particles. In  $A_xC_{60}$  alkali fullerenes the alkali atoms transfer their  $s$  electrons to  $C_{60}$  molecules. As a result the Coulomb energy becomes dominant in the formation of different ordered structures [4, 5]. At the same time these transferred electrons take part in the screening of the Coulomb interaction between two alkali ions. In the knowledge of the screening mechanism, one could derive an effective pair interaction, which is expected to be a short-range one. Unfortunately, we know of no satisfactory approach for determining the screening in these materials.

In the present model we assume a simple screening mechanism. First of all the effect of dielectric media is considered via the dielectric constant  $\epsilon$ . Furthermore, the charge of each alkali ion is completely screened by the first-neighbour  $C_{60}$  molecules. This means that there is a uniform distribution of transferred  $s$  electrons in the first-neighbour  $C_{60}$  molecules. This simplification seems also to be an appropriate approximation for a metallic system if the Thomas–Fermi length is not greater than the shortest A– $C_{60}$  distance ( $\simeq 6.3$  Å).

In accordance with the above assumption, the charge assembled on a given  $C_{60}$  molecule may vary: its value depends on the number of alkali ions residing around the molecule. A series of UHF-MNDO calculations has confirmed that the electronic energy of a solitary

$C_{60}^{x-}$  ion may be approximated as  $E(x) = a + bx + cx^2$ , where the quadratic term mediates an interaction between those alkali ions transferring charges to the same  $C_{60}$  molecule(s). This contribution may be considered as the electrostatic energy of a charged spherical shell with a radius  $R = 4.45 \text{ \AA}$ , because the term  $a + bx$  does not affect the thermodynamic behaviour. The effect of dielectric media is taken into account by means of the application of the Kirkwood–Onsager theory [6] as in I. Rabe *et al* [5] suggested such a spherical-shell model, choosing  $R = 3.5 \text{ \AA}$  (and  $\varepsilon = 1$ ) which is equivalent to the shell radius formed by the carbon nucleus of the  $C_{60}$  molecule. We use the concept of this spherical-shell model because of its descriptiveness, i.e. the electronic energy of the  $C_{60}^{x-}$  ion will be estimated as  $E(x) = (xe)^2/2\varepsilon R$ .

Without repeating the formalism introduced in I, we now concentrate on the mean-field analysis of the model using six- and two-sublattice approximations. The results are summarized in phase diagrams calculated for three different values of  $R$ . In the first case  $R$  is estimated by using the data from UHF-MNDO calculations. Accepting the suggestion of Rabe *et al* [5], in the second case, we have determined the phase diagram for  $R = 3.5 \text{ \AA}$ . Finally we have chosen an intermediate value for  $R$  in order to display a phase diagram different from the previous ones.

In the analysis of the above model we restrict ourselves to the rigid BCC structure. Our main purpose is to analyse the general features of the present model in the parameter region relevant for alkali-metal fullerides. A more rigorous comparison of the states appearing in FCC, BCC and body-centred-tetragonal (BCT) host lattices [7–10] goes beyond the scope of the present work.

## 2. The model

In BCC structures there are only tetrahedral interstitial sites for the intercalated alkali ions. To describe the distribution of  $A^+$  ions we introduce a site variable  $\eta_i$  which is 1 if the interstitial site  $i$  is occupied by an alkali ion and 0 for empty sites. The energy for any configuration of alkali ions is given by the lattice-gas Hamiltonian

$$H = \sum_i \epsilon \eta_i + \frac{1}{2} \sum_{ij} V_{ij} \eta_i \eta_j \quad (1)$$

characterized by the site energy  $\epsilon$  and the effective pair interaction  $V_{ij}$ . Both quantities are determined by assuming the screening mechanism mentioned above.

The calculation detailed in I results in an effective pair interaction dependent on the ion–ion distance  $r_{ij}$  as shown in figure 1 for  $R = 4.45 \text{ \AA}$ . Henceforth the energy is measured in units of  $e^2/(\varepsilon a)$  where  $a$  is the lattice constant. Notice that  $V_{ij}$  may take two values for certain values of  $r_{ij}$ . This effective interaction is repulsive for short distances and becomes attractive on increasing the ion–ion distance. In agreement with expectations, the strength of  $V_{ij}$  decreases rapidly with  $r_{ij}$ .

The interaction mediated by  $C_{60}^{x-}$  ion(s) gives a repulsive contribution to the total pair interaction until  $r_{ij}$  exceeds a threshold value. Obviously, the strength of this contribution increases when decreasing  $R$ .

In the present model the site energy may be easily determined:

$$\varepsilon = -1.3752 \frac{e^2}{\varepsilon a} + \frac{e^2}{8\varepsilon R}. \quad (2)$$

In the knowledge of the model parameters we are able to determine the energy of each ordered particle distribution. For this purpose the tetrahedral interstitial sites are divided

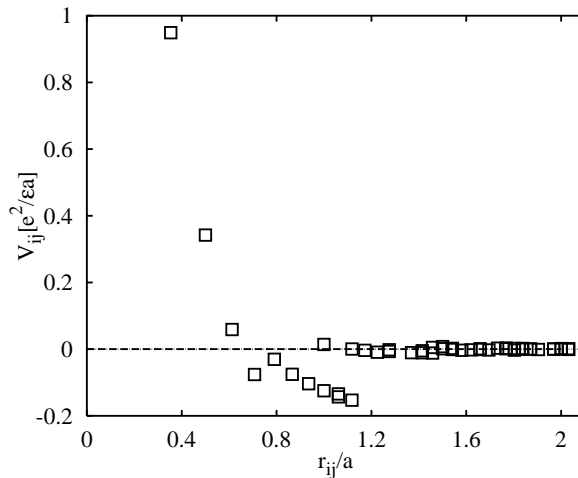


**Figure 1.** The effective pair interaction versus the ion-ion distance for  $R = 4.45 \text{ \AA}$ .

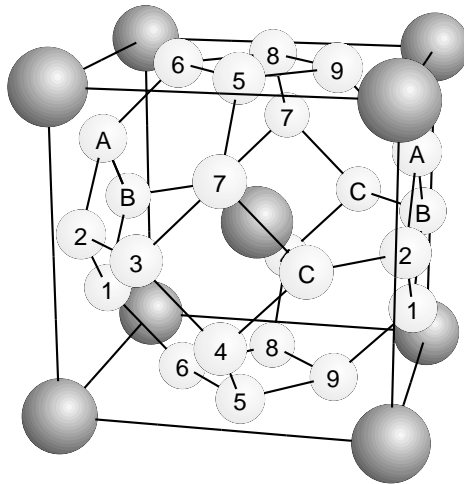


**Figure 2.** The tetrahedral interstitial sites of the BCC lattice are divided into 12 sublattices.

into 12 simple cubic sublattices indicated by hexadecimal codes from 1 to C as illustrated in figure 2.

Within this sublattice division we can distinguish  $2^{12}$  ordered states in which the sites belonging to the same sublattice are uniformly occupied or empty. Figure 3 shows the energies per  $C_{60}$  of these states as a function of the alkali content  $x$ . Here it is worth mentioning that the charges of the  $C_{60}$  molecules are uniform within an ordered state. Consequently, the energies plotted in figure 3 are the sums of the corresponding Madelung energy and the estimated electronic energy of  $C_{60}$ .

Figure 3 demonstrates clearly that this model has only three stable ordered structures if  $R = 4.45 \text{ \AA}$ . For the stable  $x = 0$  ( $x = 6$ ) state all of the tetrahedral sites are empty (occupied). In the half-filled system ( $x = 3$ ) the stable state is equivalent to the well known A15 structure, i.e. the sublattices 2, 4, 6, 7, 9 and B are completely occupied whereas the rest of the sites are empty. If the equivalent sublattices are combined, the formation of this

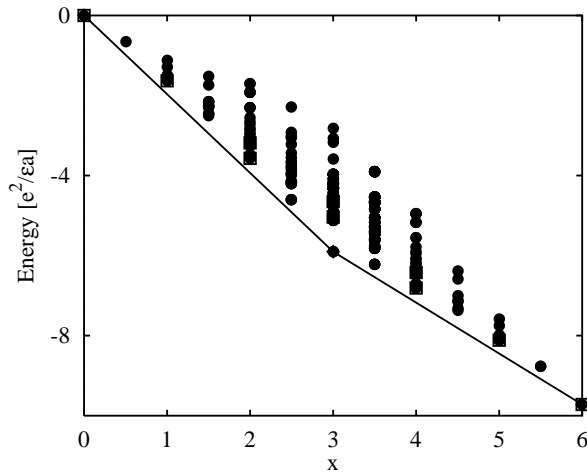


**Figure 3.** The energy of the 12-sublattice ordered states as a function of alkali-metal content for  $R = 4.45 \text{ \AA}$ . The black diamonds and squares refer to states described by the two- and six-sublattice formalisms. The solid line connects the stable phases.

structure may be well described by using a much simpler two-sublattice formalism.

The states with the minimum energy for  $x = 1, 2, 4$  and  $5$  exhibit additional symmetry; more precisely, the occupations in sublattices  $\alpha$  and  $\alpha + 6$  are equivalent for  $\alpha = 1, \dots, 6$ . The combination of the equivalent sublattices results in the six-sublattice formalism studied previously [11]. In this case the tetrahedral sites are divided into six interpenetrating BCC sublattices; therefore the translation symmetry of the host lattice remains valid in the above-mentioned states. The role of these states becomes important when studying the system for lower  $R$ .

The decrease of  $R$  gives an  $x$ -dependent contribution to the energies (see figure 3) without modifying the energy differences for fixed  $x$ . The minimum-energy states for  $x = 1$  and  $5$  become stable if  $R/a < 0.3411$ . The simultaneous appearance of the stable states for  $x = 1$  and  $5$  is a consequence of the particle-hole symmetry. In the  $x = 1$  stable state only the sites of one of the six sublattices are occupied. If  $R/a < 0.3342$  then the system exhibits stable states for  $x = 2$  and  $4$ . In the  $x = 2$  stable state the simultaneous occupation of the first-neighbour sites is excluded.

The above ground-state investigations support the assertion that the mean-field analysis may be restricted to the two- and six-sublattice approximations.

### 3. Mean-field approximation

The six-sublattice mean-field approximation was previously introduced to describe the ordering processes in superionic AgI where the  $\text{I}^-$  ions form a BCC cage lattice for the mobile  $\text{Ag}^+$  ions [11]. This sublattice division is obvious because the number of tetrahedral interstitial sites is just six times the number of points in the BCC host lattice. In this approach, the equilibrium states are characterized by the average sublattice occupations  $\sigma_\nu$  ( $\nu = 1, \dots, 6$ ). The energy per  $\text{C}_{60}$  molecule is expressed in terms of these quantities as

$$\mathcal{H} = \sum_{\nu} \varepsilon \sigma_{\nu} + \frac{1}{2} \sum_{\nu, \tau} J_{\nu\tau} \sigma_{\nu} \sigma_{\tau} \quad (3)$$

where  $\varepsilon$  is defined by equation (2) and the mean-field coupling constants  $J_{\nu\tau}$  summarize the effective interactions ( $V_{ij}$ ) between a site of sublattice  $\nu$  and all of the sites belonging to sublattice  $\tau$ . Due to the symmetries of this sublattice structure there are only three independent mean-field coupling constants [11]. The numerical calculations yield

$$\begin{aligned} J_{11} = \dots = J_{66} &= -1.16445 \frac{e^2}{\varepsilon a} \\ J_{12} = \dots = J_{65} &= +0.08251 \frac{e^2}{\varepsilon a} \\ J_{14} = \dots = J_{63} &= -0.30468 \frac{e^2}{\varepsilon a} \end{aligned} \quad (4)$$

if  $R = 4.45 \text{ \AA}$ .

In the second approach we distinguish only two sublattices ( $\alpha$  and  $\beta$ ) as described in the previous section. Now the mean-field energy per  $C_{60}$  molecule is defined by the following expression:

$$\mathcal{H} = 3 \sum_r \varepsilon \sigma_r + \frac{3}{2} \sum_{r,s} J'_{rs} \sigma_r \sigma_s \quad (5)$$

where  $r, s = \alpha, \beta$  and the values of  $J'_{rs}$  are determined numerically for the same radius:

$$\begin{aligned} J'_{\alpha\alpha} = J'_{\beta\beta} &= -1.83360 \frac{e^2}{\varepsilon a} \\ J'_{\alpha\beta} = J'_{\beta\alpha} &= +0.69451 \frac{e^2}{\varepsilon a}. \end{aligned} \quad (6)$$

Within this formalism the twofold-degenerate A15 structure is given as  $\sigma_\alpha = (1 - \sigma_\beta) = 0$  or 1. Obviously, the energies of the empty ( $\sigma_\alpha = \sigma_\beta = 0$ ) and completely occupied ( $\sigma_\alpha = \sigma_\beta = 1$ ) states are equivalent to those suggested by the six-sublattice formalism.

Using the same method, one can also evaluate the mean-field coupling constants of the 12-sublattice approximation. The values of these parameters are, of course, strongly related

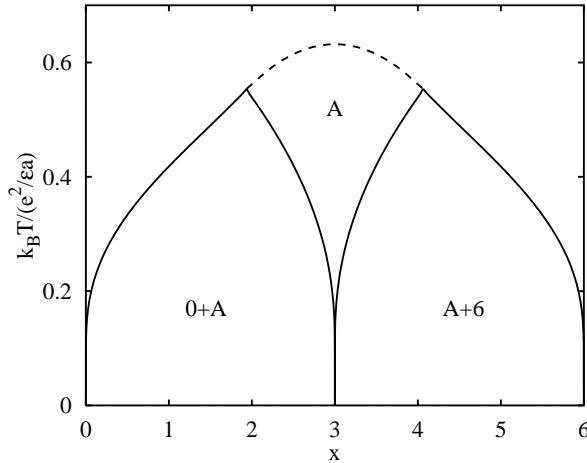


**Figure 4.** The phase diagram suggested by mean-field approximation for  $R = 4.45 \text{ \AA}$ . The dashed line represents a continuous two-sublattice ordering process. The phases are labelled with the alkali contents of the ordered states.

to the previous ones defined by equations (4) and (6). More precisely,  $J_{v\tau}$  and  $J'_{rs}$  are the linear combinations of the mean-field coupling constants of the 12-sublattice approximation.

The equilibrium state characterized by sublattice occupations is determined by minimizing the Gibbs potential for fixed temperature and chemical potential. Following I, the results of this mean-field analysis are summarized in phase diagrams.

In agreement with the particle-hole symmetry, the phase diagrams are also symmetric, as illustrated in figure 4. In this figure the dashed line represents the critical temperature of the continuous sublattice ordering from the high-temperature ( $\sigma_\alpha = \sigma_\beta$ ) distribution towards the A15 structure. Below the critical temperature,  $\sigma_\alpha$  differs from  $\sigma_\beta$  and the alkali content per  $C_{60}$  molecule is given as  $x = 3(\sigma_\alpha + \sigma_\beta)$ . In the subsequent phase diagrams this state is denoted as A, referring to the symmetry of the A15 structure.

The two-sublattice ordering process is analogous to the formation of antiferromagnetic order in Ising models. The critical (Néel) temperature may be expressed in terms of the coupling constants as a function of  $x$ ; that is,

$$k_B T_N = \frac{x(6-x)}{36} (J'_{\alpha\beta} - J'_{\alpha\alpha}). \quad (7)$$

This transition temperature has a maximum at  $x = 3$  and vanishes when  $x$  goes to 0 or 6. Accepting the numerical value  $\varepsilon = 9$  deduced by Sanguinetti and Benedek [12] from the charge-induced vibrational shift, the above expression predicts  $T_N \approx 1000$  K for  $x = 3$ . Instead of this continuous transition, at low temperatures the system segregates into two phases with different alkali contents (indicated by solid lines in figure 4). The values given refer to the alkali contents in the ordered states at  $T = 0$ .

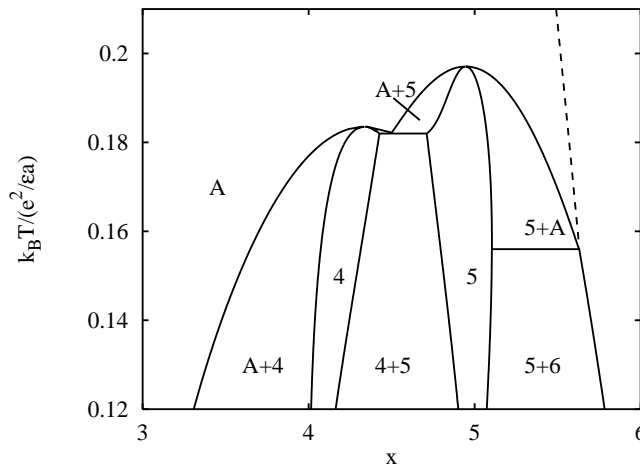


**Figure 5.** The phase diagram in the mean-field approximation for  $R = 3.5 \text{ \AA}$  exhibits a eutectoid phase transition at  $x \simeq 4.5$ .

We have determined the phase diagram for  $R = 3.5 \text{ \AA}$  ( $R/a = 0.303$ ), suggested by Rabe *et al* [5]. In this case only half ( $3 \leq x \leq 6$ ) of the symmetric phase diagram is represented in figure 5.

This figure shows stable ordered structures for  $x = 3, 4, 5$  and  $6$  at low temperatures. The  $x = 3$  state transforms continuously to the random distribution with a critical temperature given by equation (7). A part of this curve is denoted by the dashed line in figure 5. As demonstrated, state A can exist for a wide range of  $x$ . The ordered structures with nominal compositions  $x = 4$  and  $5$  become unstable upon increasing the temperature above

$k_B T_4 = 0.1835e^2/(\epsilon a)$  and  $k_B T_5 = 0.1971e^2/(\epsilon a)$ . Furthermore, the model exhibits a eutectoid phase transition at  $x \approx 4.5$ . This phenomenon implies the stability of an ordered structure with  $x = 4.5$  for smaller  $R$ .

Here it is worth mentioning that the cubic symmetry is broken in the ordered structures if  $x = 1, 2, 4$  and  $5$ . It seems reasonable to suggest that a distortion of the host lattice occurs because of the breaking of cubic symmetry related to the ordering process. A similar phenomenon was investigated by O'Sullivan *et al* [13] and by Seok and Oxtoby [14] when studying the ordering process in the superionic phase of AgI.

As mentioned above, there exists a very narrow range of  $R$  where the ordered state  $x = 5$  is observable whereas the state  $x = 4$  is unstable. In order to illustrate typical behaviour within this region, we have evaluated the phase diagram for  $R/a = 0.337$ .

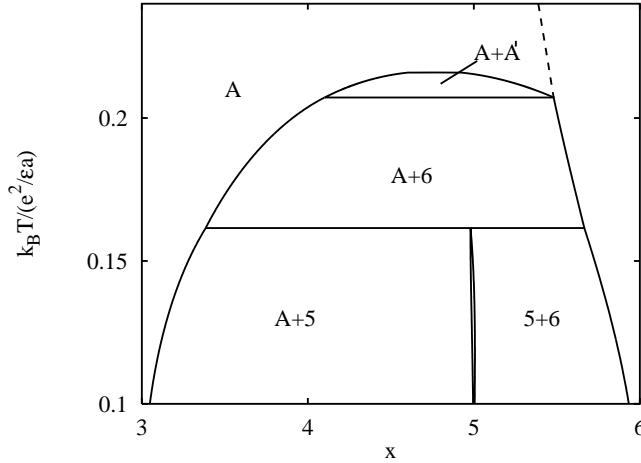


**Figure 6.** The phase diagram for  $R/a = 0.337$ .

In figure 6 the dashed line refers to the critical temperature of the continuous sublattice ordering described above. In this phase diagram there is a region denoted as  $A + A'$  where two A phases coexist with different compositions. At lower temperatures (see region  $A + 6$ ) the difference between  $\sigma_\alpha$  and  $\sigma_\beta$  disappears for large alkali content ( $x \simeq 5.5$ ). State 5 (with five of six occupied sublattices) becomes stable if  $k_B T < 0.1615e^2/(\epsilon a)$ .

The above series of phase diagrams display the electronic energy effect of the  $C_{60}^{x-}$  ion on the thermodynamic behaviour. In contrast to the early experiments and calculations, the present model suggests the appearance of state 5 if state 4 is stable. Very recently, however, Lof *et al* [15] found a local minimum near  $x = 5$  when measuring the temperature- and concentration-dependent conductivity of potassium-doped  $C_{60}$  films. This observation may be interpreted as an experimental indication of the existence of such a state. Here it is emphasized that this state is sixfold degenerate and therefore a polydomain structure is expected to appear in experiments.

#### 4. Summary and conclusions

Using two- and six-sublattice mean-field approximations we have studied a lattice-gas model of intercalation alloys in which the Coulomb interaction between the intercalated elements is screened out by the charges distributed on the BCC host lattice. We have assumed that the intercalated particle residing in a tetrahedral interstitial position transfers  $e/4$  charges to



the (four) nearest-neighbour host-lattice molecules. The energy of the charged host-lattice molecule is treated as the electrostatic energy of a charged spherical shell of radius  $R$ . The family of alkali fullerides is the best candidate as regards satisfying the above conditions. This fact has motivated the choice of parameters when determining the thermodynamic behaviour suggested by this model. Although our analysis is restricted to alkali fullerides, we can derive predictions for alkaline earths if  $2e$  is substituted for  $e$  in all of the formulae, including the energy unit in the figures.

The model takes the electrostatic interactions into consideration exactly, at zero temperature, i.e. it reproduces the Madelung energies for the ordered structures. Owing to its simplicity, the model has only two parameters: the lattice constant is taken from experiments and the value of  $R$  is estimated from a series of UHF-MNDO calculations. In this case the model suggests only three stable ordered structures. Besides the empty ( $x = 0$ ) and fully occupied ( $x = 6$ ) states we have found a stable A15 structure ( $x = 3$ ). The fully occupied ( $x = 6$ ) state is observed experimentally for  $A = K, Rb$  and  $Cs$ . For smaller-atom alkali elements ( $Li, Na$ ), however, the interstitial voids are too large compared with the ionic sizes. Yildirim *et al* [16] suggest clusters of four to nine sodium atoms inside the octahedral voids of the FCC lattice. The structure of  $Na_6C_{60}$  exhibits an FCC host lattice with single occupation of tetrahedral sites and fourfold filling of the octahedral voids [17]. Obviously, the description of these former structures goes beyond the range of validity of the present lattice-gas formalism.

According to the electrostatic force calculations, the FCC structure is preferable to the BCC one for  $x \leq 3$  [4, 5]. This theoretical prediction agrees with experiments [2, 3]. Up till now only the  $Ba_3C_{60}$  compound has been found to exhibit the A15 structure [18].

In the present model the robust A (A15) state can exist over wide ranges of temperature and alkali content as indicated in the phase diagrams. By the analogy with antiferromagnetic ordering, this particle arrangement transforms continuously to the random distribution when the temperature is increased.

The most surprising prediction of the present calculation is that of the existence of the  $A_5C_{60}$  phase when the  $A_4C_{60}$  compound is stable. In these ordered structures the cubic symmetry is broken and therefore lattice distortions are expected to accompany the ordering processes. For example, the  $A_4C_{60}$  compounds have been observed with BCT structure [4] which may be considered as a distorted BCC lattice with four out of six sublattices to be occupied. The present model permits the existence of the stable  $A_4C_{60}$  compounds together with  $A_5C_{60}$  ones if  $R/a < 0.334$ . Recently the electronic structure of  $Ba_5C_{60}$  has been analysed theoretically [19] although this structure has not been detected experimentally. The breaking of the cubic symmetry in these former states raises many questions related to the role of lattice distortion.

## Acknowledgments

We wish to acknowledge support from the Hungarian National Research Fund (OTKA) under Grants No T16734 and No F14378.

## References

- [1] Udvardi L and Szabó G 1996 *J. Phys.: Condens. Matter* **8** 10970
- [2] Fischer J E and Heiney P A 1993 *J. Phys. Chem. Solids* **54** 1725
- [3] Weaver J H and Poirier D M 1994 *Solid State Physics* vol 48 (New York: Academic) p 1
- [4] Fleming R M *et al* 1991 *Nature* **352** 701

- [5] Rabe K M, Phillips J C and Vandenberg J M 1993 *Phys. Rev. B* **47** 13 067
- [6] Bottcher C J 1952 *Theory of Electric Polarization* (Amsterdam: Elsevier)
- [7] Zhu Q, Zhou O, Coustel N, Vaughan G B M, McCauley J P, Romanov W J, Fischer J E and Smith A B 1991 *Science* **254** 545
- [8] Stephens P W and Mihaly L 1992 *Phys. Rev. B* **45** 543
- [9] Poirier D M, Ohno T R, Kroll G H, Benning P J, Stepniak F, Weaver J H, Chibante L P F and Smalley R E 1993 *Phys. Rev. B* **47** 9870
- [10] Pichler T, Winkler R and Kuzmany H 1994 *Phys. Rev. B* **49** 15 879
- [11] Szabó G 1986 *J. Phys. C: Solid State Phys.* **19** 3775
- [12] Sanguinetti S and Benedek G 1994 *Phys. Rev. B* **50** 15 439
- [13] O'Sullivan K, Chiarotti G and Madden P A 1991 *Phys. Rev. B* **43** 13 536
- [14] Seok C and Oxtoby D W 1997 *Phys. Rev. B* **56** 11 485
- [15] Lof R W, Jonkman H T and Sawatzky G A 1995 *Solid State Commun.* **93** 633
- [16] Yildirim T, Zhou O, Fischer J E, Bykovetz N, Stronglin R A, Cichy M A, Smith A B III, Lin C L and Jelinek R 1992 *Nature* **360** 568
- [17] Rosseinsky M J, Murphy D W, Fleming R M, Tycko R, Ramirez A P, Siegrist T, Dabbagh G and Barrett S E 1992 *Nature* **356** 416
- [18] Kortan A R, Kopylov N, Fleming R M, Zhou O, Thiel F A, Haddon R C and Rabe K M 1993 *Phys. Rev. B* **47** 13 070
- [19] Shedel-Niedrig T, Böhm M C, Werner H, Schulte J and Schlögl R 1997 *Phys. Rev. B* **55** 13 542